Neuro-fuzzy control strategy for an offshore steel jacket platform subjected to wave-induced forces using magnetorheological dampers [†]

Atabak Sarrafan[*], Seiyed Hamid Zareh, Amir Ali Akbar Khayyat and Abolghassem Zabihollah

School of Science and Engineering, Sharif University of Technology, Iran

---

Abstract

Magnetorheological (MR) damper is a prominent semi-active control device to vibrate mitigation of structures. Due to the inherent non-linear nature of MR damper, an intelligent non-linear neuro-fuzzy control strategy is designed to control wave-induced vibration of an offshore steel jacket platform equipped with MR dampers. In the proposed control system, a dynamic-feedback neural network is adapted to model non-linear dynamic system, and the fuzzy logic controller is used to determine the control forces of MR dampers. By use of two feedforward neural networks required voltages and actual MR damper forces are obtained, in which the first neural network and the second one acts as the inverse dynamics model, and the forward dynamics model of the MR dampers, respectively. The most important characteristic of the proposed intelligent control strategy is its inherent robustness and its ability to handle the non-linear behavior of the system. Besides, no mathematical model needed to calculate forces produced by MR dampers. According to linearized Morison equation, wave-induced forces are determined. The performance of the proposed neuro-fuzzy control system is compared with that of a traditional semi-active control strategy, i.e., clipped optimal control system with LQG-target controller, through computer simulations, while the uncontrolled system response is used as the baseline. It is demonstrated that the design of proposed control system framework is more effective than that of the clipped optimal control scheme with LQG-target controller to reduce the vibration of offshore structure. Furthermore, the control strategy is very important for semi-active control.

Keywords: Clipped optimal control system; Magnetorhelogical damper; Neuro-fuzzy control strategy; Semi-active control; Wave-induced vibration

---

1. Introduction

In modern world, oil crisis has become a bottle-neck of economy. Therefore the offshore structures, especially the oil and gas production platforms, play a more and more important role. The environment surrounding offshore platforms is harsh and complicated. A schematic of sample offshore steel jacket platform under environmental loading is illustrated in Fig. 1. As well as erosion from sea water, they may have to endure strong dynamic forces caused by wind, sea wave, sea current, sea ice and even earthquake. Therefore, the structural safety and durability of offshore platforms have raised great concerns of oil industry. To prevent fatigue damage, to ensure safety and production efficiency and to make people on the platform comfortable, displacement and acceleration of the platforms should be limited. Many control schemes have been studied to suppress the vibration of offshore structures [1-9]. Considering issues of control system reliability and power supply, pas-
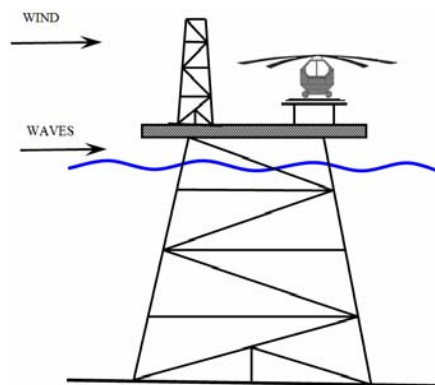

Fig. 1. Environmental loading on offshore steel jacket platform.

sive [5-8] and semi-active control [9] are more appealing than active one [1-4].

Recently, semi-active control systems have attracted a great deal of attention in civil engineering field, because they offer the adaptability of active control devices while without requiring large power sources. The MR damper is a new kind of semi-active control device which utilizes the essential charac-

teristic of MR fluids being their ability to reversibly change from free-flowing, linear viscous liquids to semi-solids having controllable yield strength in milliseconds when exposed to magnetic field. At the same time it has merits of simple construction, cheap cost and excellent control effect thereby gaining more attention. When structures deform due to vibration, MR dampers will adjust their characteristic parameters in accordance with given control laws and will absorb vibration energy. From this point of view, structural vibration control using MR dampers is one of the most promising fields in civil engineering, and a wide range of theoretical and experimental studies have been performed to assess the efficacy of MR dampers [10-15]. Recent tests of a 20-ton MR damper at the University of Notre Dame have demonstrated that these devices can provide forces of the magnitude required for full-scale structural control applications [16].

Because MR dampers are highly non-linear devices, developing control algorithms to fully take advantage of their characteristics has been challenging. Several control strategies have been proposed to use with these devices [16, 18-43], and as shown in Ref. [17], they can be categorized as model-based control, that is, algorithms that require an accurate mathematical model of the system and intelligent control. The performance of some of the control systems proposed has been compared through simulations [12, 20, 30].

Although model-based control strategies have been successful to reduce structural vibrations, all models developed are based on assumptions and uncertainties which can greatly affect their accuracy, and therefore influence controller's performance. One must, therefore, make sure that these model-based controllers are robust enough to control the real life structures. The non-linear nature and complexity of systems have also lead to the creation of sophisticated models which are often computationally intensive, and therefore difficult and sometimes even impractical to use in the development of control strategies. Intelligent technology-based control has therefore been suggested as an alternative to strategies that rely on system model. Three main categories of intelligent control algorithms have been proposed to use with the MR dampers: neural network-based control, fuzzy logic-based control and neuro-fuzzy based control.

Neural network and fuzzy controller techniques can offer a simple and robust framework for specification of non-linear control laws that can accommodate uncertainty and imprecision. In recent years, neural network and fuzzy control techniques are used widely for the semi-active vibration control in civil engineering. In the category of neuro-control, Ni et al. [34] proposed a neuron-control method for semi-active vibration control of stay cables using MR dampers. The analysis results showed that the proposed control strategies could effectively implement semi-active vibration control of stay cables with the use of MR dampers. Shiraishi et al. [35] proposed an adaptive neural network to control a three-story structural model equipped with a prototype damper they designed and constructed. Numerical simulations and experiments, which showed good agreement, verified the perform-

ance of their proposed control strategy. Based on neural networks, Dalei and Jianqiang [36] employed an indirect adaptive control strategy to control MR dampers on base isolated structures. They used back propagation algorithm with momentum term to train the weights of two used neural networks. Through numerical simulation they showed that the proposed strategy is more effective than the use of a neural network controller without quadratic momentum term. Xu et al. [37] proposed the use of neural networks to control MR dampers. Numerical simulation results on a three-story reinforced concrete structure model showed that this control method is more effective than the traditional elastoplastic time-history analysis method. In the category of fuzzy-control, Wang [38] described an adaptive fuzzy control strategy that Zhou et al. [39] successfully applied for control of linear and non-linear structures. They showed that the adaptive feature of a fuzzy controller has multiple advantages in controlling a building that has an MR damper system. Yan and Zhou [40] presented a design strategy based on genetic algorithm (GA) for semi-active fuzzy control of structures that have MR dampers installed to prevent damage from severe dynamic loads such as earthquakes. They employed GA as an adaptive method for design of the fuzzy controller, which is known as a genetic adaptive fuzzy (GAF) controller. They showed the effectiveness and efficiency of their proposed intelligent control strategy using numerical simulations for single and multiple damper cases. Ok et al. [41] proposed a semi-active fuzzy control technique to enhance the seismic performance of cable-stayed bridges using MR dampers. They designed the fuzzy logic controller to directly determine the input voltage of an MR damper from the response of the MR damper. They proved that their proposed semi-active fuzzy control technique can effectively mitigate the seismic response of cable-stayed bridges and successfully enhance the robust performance of the MR damper system. In the category of neuro-fuzzy control, Xu and Guo [42] proposed neuro-fuzzy control strategy, in which the neural-network technique is adopted to solve time-delay problem and the fuzzy controller is used to determine the control current of MR dampers quickly and accurately. Through a numerical example, they proved that the control effect of the neuro-fuzzy control strategy is better than that of the bi-state control strategy. Schurter and Roschke [43] presented a neuro-fuzzy technique to reduce the environmentally-induced vibration of two types of MR-building models. They developed a correlation between accelerations of the building (fuzzy controller input) and voltage applied to the MR damper (fuzzy controller output). The developed correlation formed the basis of their proposed intelligent neuro-fuzzy control strategy. According to numerical simulation, they showed that MR dampers are less effective control mechanisms than passive dampers with respect to a single degree of freedom (DOF) building model. Moreover, MR dampers are superior when used with multiple DOF structures to reduce the lateral acceleration.

The previous studies made full use of the advantages of the neural network and the fuzzy logic, and solved the different

problems which lay in the civil engineering structures. Few researches involved combination of the two techniques to solve the inherent non-linear nature problem of the MR damper to generate ideal damping force for vibration control of offshore structures under wave-induced forces. In current research, the control objective is to reduce both the displacement response that determines the structural safety and the acceleration response that reflects the comfort level of occupants. In this paper, four MR dampers are added in an offshore steel jacket platform [44]. For the intelligent structure under wave loading, a dynamic-feedback neural network is adapted to model non-linear dynamic system and the fuzzy logic controller is used to determine the control forces of MR dampers. Required voltages and actual MR damper forces are obtained by use of two feedforward neural networks, in which the first neural network and second one act as the inverse dynamics model and the forward dynamics model of the MR dampers, respectively. In order to verify the effectiveness of the proposed neuro-fuzzy control strategy, the uncontrolled structure and the semi-actively controlled using clipped optimal control algorithm structure are compared with the neuro-fuzzy controlled structure. Through a numerical example, it can be concluded that the control strategy is very important for semi-active control, and the control effect of the neuro-fuzzy control strategy is better than that of the clipped optimal control strategy with LQG-target controller.

2. Modeling of an offshore steel jacket platform

In this paper, finite element method (FEM) is utilized to model an offshore steel jacket platform. The FEM provides a practical and less expensive way to study the dynamic response of offshore structures under environmental loadings. General beam element or simply frame element is used in this research. The frame element is seen to posses the properties of both truss and beam elements. In fact, the frame structures can be found in most of our real world structural problems, for there are not many structures that deform and carry loadings purely in neither axial directions nor purely in transverse directions.

In a planar frame element, there are 3 DOFs at each node in local coordinate system. They are the axial deformation in the x direction, u, deflection in y direction, v, and the rotation in the x–y plane and with respect to the z-axis, θ_z. Therefore, each element with two nodes has a total of 6 DOFs. Displacement and rotation components at node i are u_i, v_i and θ_{zi}, $i = 1, 2$. DOFs of a frame element are shown in Fig. 2.

The forces and displacements in local coordinate system are related by use of Eq. (1) [45].

$$\begin{Bmatrix} f_{x1} \\ f_{y1} \\ M_1 \\ f_{x2} \\ f_{y2} \\ M_2 \end{Bmatrix} = k_e \begin{Bmatrix} u_1 \\ v_1 \\ \theta_{z1} \\ u_2 \\ v_2 \\ \theta_{z2} \end{Bmatrix} \qquad (1)$$
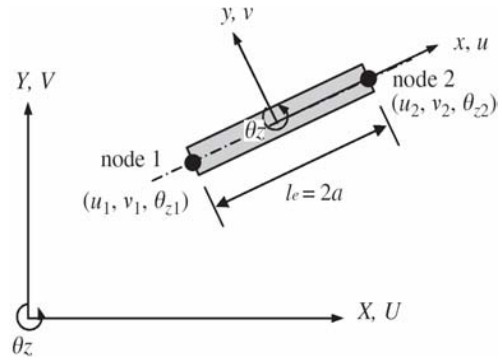

Fig. 2. DOFs of a planar frame element [45].

where

$$k_e = \begin{bmatrix} \frac{AE}{2a} & 0 & 0 & -\frac{AE}{2a} & 0 & 0 \\ 0 & \frac{3EI_z}{2a^3} & \frac{3EI_z}{2a^2} & 0 & -\frac{3EI_z}{2a^3} & \frac{3EI_z}{2a^2} \\ 0 & \frac{3EI_z}{2a^2} & \frac{2EI_z}{a} & 0 & -\frac{3EI_z}{2a^2} & \frac{EI_z}{a} \\ -\frac{AE}{2a} & 0 & 0 & \frac{AE}{2a} & 0 & 0 \\ 0 & -\frac{3EI_z}{2a^3} & -\frac{3EI_z}{2a^2} & 0 & \frac{3EI_z}{2a^3} & -\frac{3EI_z}{2a^2} \\ 0 & \frac{3EI_z}{2a^2} & \frac{EI_z}{a} & 0 & -\frac{3EI_z}{2a^2} & \frac{2EI_z}{a} \end{bmatrix}. \qquad (2)$$

In Eq. (1), f_{xi}, f_{yi}, are forces applied to node i in x and y direction, respectively, M_i are moment applied to node i, $i = 1, 2$, k_e is a 6×6 stiffness matrix of each element in local coordinate system. In stiffness matrix k_e, A is cross sectional area of the element, l_e is the element length $= (2a)$, I_z is the moment of inertia of the cross section of the beam with respect to z-axis, E is Young's modulus of element. The 6×6 mass matrix of each element m_e in local coordinate system is stated in Eq. (3).

$$m_e = \frac{\rho A a}{105} \begin{bmatrix} 70 & 0 & 0 & 35 & 0 & 0 \\ 0 & 78 & 22a & 0 & 27 & -13a \\ 0 & 22a & 8a^2 & 0 & 13a & -6a^2 \\ 35 & 0 & 0 & 70 & 0 & 0 \\ 0 & 27 & 13a & 0 & 78 & -22a \\ 0 & -13a & -6a^2 & 0 & -22a & 8a^2 \end{bmatrix} \qquad (3)$$

where ρ is mass density of the element. Transformation matrix **T**, which relates matrices in local coordinate system to global ones, is introduced in Eq. (4).

$$T = \begin{bmatrix} \cos\alpha & \sin\alpha & 0 & 0 & 0 & 0 \\ -\sin\alpha & \cos\alpha & 0 & 0 & 0 & 0 \\ 0 & 0 & 1 & 0 & 0 & 0 \\ 0 & 0 & 0 & \cos\alpha & \sin\alpha & 0 \\ 0 & 0 & 0 & -\sin\alpha & \cos\alpha & 0 \\ 0 & 0 & 0 & 0 & 0 & 1 \end{bmatrix} \qquad (4)$$
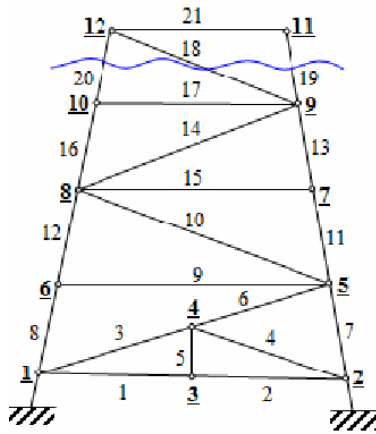
Fig. 3. A fixed offshore steel jacket platform [44].

Table 1. Geometric properties of cylindrical steel members of offshore platform.

Element No.	Outside diameter (m)	Length (m)	Thickness (mm)	α (°)
1	0.457	8.1415	10	0
2	0.457	8.1415	10	180
3	0.273	8.20	7	90
4	0.273	11.555	7	130.94
5	0.273	11.555	7	45.205
6	0.273	10.019	7	45.205
7	0.559	15.2897	11	93.86
8	0.559	15.2897	11	86.145
9	0.356	14.137	8	180
10	0.457	18.704	10	134.87
11	0.559	13.256	11	93.86
12	0.559	13.256	11	86.145
13	0.324	12.256	8	180
14	0.457	16.216	10	45.13
15	0.406	11.492	9	93.86
16	0.406	11.492	9	86.145
17	0.324	10.625	8	180
18	0.381	14.058	8	134.87
19	0.406	9.963	9	93.86
20	0.406	9.963	9	86.145
21	0.381	9.212	8	180

where α is the angle between the x-axis of local and X-axis of global coordinating systems.

Eqs. (5) and (6) are used to transform the stiffness and mass matrices of each frame element into global coordinate system. In the same manner, the force vector applied to the frame element is transformed into the global coordinate system by Eq. (7).

$$K_e = T^T k_e T \qquad (5)$$

$$M_e = T^T m_e T \qquad (6)$$

$$F_e = T^T f_e \qquad (7)$$

The structural model of a fixed offshore steel jacket platform is illustrated in Fig. 3.

The geometric properties of offshore steel jacket platform are in Table 1 [44].

3. Modeling of wave-induced forces

Offshore structures are exposed to non-linear hydrodynamic forces. The non-linearity of these forces arises from their dependence on the flexibility of the structure which induces a self-excited load term [46]. The fluid forces acting on a cylinder, considering the relative motion of body in the fluid is modeled using the well-known Morison Eq. [47]. For an element of a cylinder element, this equation is [48]

$$df_w = \rho_w dV C_M \dot{q}_n + \frac{1}{2}\rho C_D dA |q_n - \dot{x}_n|(q_n - \dot{x}_n) \qquad (8)$$

where df_w is wave force per unit length of the member, C_D and C_M are drag and inertia coefficients, respectively, dV and dA are displaced volume of the member and projected area normal to the member axis, ρ_w is the mass density of water, q_n and $\dot{q}_n$ infer to the time dependent velocity and acceleration of the fluid normal to member axis at joint n, respectively, $\dot{x}_n$ is the absolute velocity of joint n, and $(q_n - \dot{x}_n)$ is the relative water velocity at joint n. Velocity and acceleration of water particle

can be derived according to relevant wave theories. Stokes second order wave theory is utilized to calculate the horizontal and vertical water particle velocity and acceleration [49, 50]

$$u = \frac{H\pi}{T}\frac{\cosh k(y+d)}{\sinh kd}\cos(kx - \omega t) \qquad (9)$$
$$+ \frac{3H^2\pi^2}{4T\lambda}\frac{\cosh k(y+d)}{\sinh^4 kd}\cos[2(kx - \omega t)]$$

$$\dot{u} = \frac{2H\pi^2}{T^2}\frac{\cosh k(y+d)}{\sinh kd}\sin(kx - \omega t) \qquad (10)$$
$$+ \frac{3H^2\pi^3}{T^2\lambda}\frac{\cosh 2k(y+d)}{\sinh^4 kd}\sin[2(kx - \omega t)]$$

$$v = \frac{H\pi}{T}\frac{\sinh k(y+d)}{\sinh kd}\sin(kx - \omega t) \qquad (11)$$
$$+ \frac{3H^2\pi^2}{4T\lambda}\frac{\sinh 2k(y+d)}{\sinh^4 kd}\sin[2(kx - \omega t)]$$

$$\dot{v} = -\frac{2H\pi^2}{T^2}\frac{\sinh k(y+d)}{\sinh kd}\cos(kx - \omega t) \qquad (12)$$
$$- \frac{3H^2\pi^3}{T^2\lambda}\frac{\sinh 2k(y+d)}{\sinh^4 kd}\cos[2(kx - \omega t)]$$

where u and $\dot{u}$ are horizontal water particle velocity and acceleration, respectively, v and $\dot{v}$ are vertical water particle velocity and acceleration, respectively, x and y are the location of
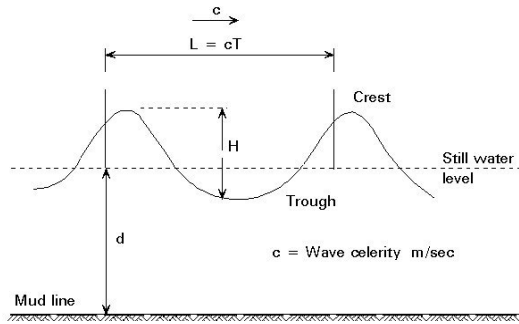
Fig. 4. Wave symbols [49].

each joint with respect to a fixed reference, H is wave height, T is wave period, k is the wave number $= (2\pi/\lambda)$, λ is the wave length, ω is the wave frequency, d is the water depth, and t is the time. Wave symbols are shown in Fig. 4.

It should be noted that there are various sources of inaccuracies in Eq. (8), e.g. from the use of constant values for C_D and C_M, which are, in fact, frequency and depth dependent. As can be observed, Eq. (8) considers the non-linear self-excited and drag forces. Using a stochastic linearization technique the Morison equation is thus approximated as [49]:

$$df_w = \rho_w dV C_M \dot{q}_n + \frac{1}{2}\rho C_D dA \sqrt{\frac{8}{\pi}}\sigma_{vr}(q_n - \dot{x}_n) \qquad (13)$$

where σ_{vr} is the Root Mean Squares (RMS) values of the relative velocity between water particles and the structure at each joint. The values at each step are obtained from the relative velocity up to the previous time step [51]. In this paper, Eq. (13) is utilized to simulate the wave hydrodynamic forces.

4. Motion equations for offshore structures with MR dampers

4.1 Mathematical model of MR dampers

In recent years, smart structures have been adopted from many engineering fields because the performance of structural systems can be improved without either significantly increasing the structure mass or requiring high cost of control power. They may be called intelligent structures, adaptive structures, active structures and the related technologies adaptronics, structronics, etc. These terminologies refer to a smart structure which is an integration of actuators, sensors, control units, and signal processing units with a structural system. The materials that are usually used to implement the smart structure are: piezoelectrics, shape memory alloys, electrostrictive/magnetostrictive materials, polymer gels, etc. [52].

Generally, an MR damper consists of a hydraulic cylinder, magnetic coils, and MR fluids that consist of micron-sized magnetically polarizable particles floating within oil-type fluids as shown in Fig. 5. The MR damper is operated as a passive damper; however, when a magnetic field is applied to the MR damper fluids, the MR fluids are changed into a semi-
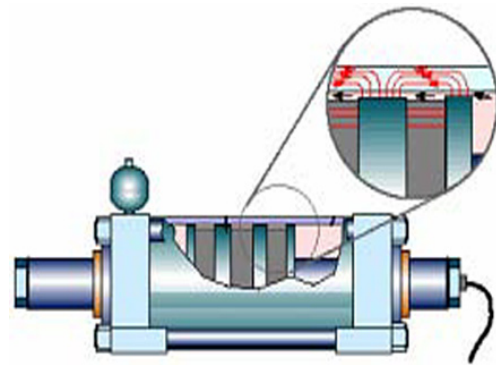

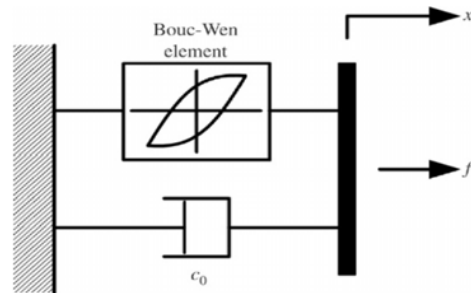Fig. 5. Schematic of the prototype 20-ton large scale MR damper [33].

Fig. 6. Mechanical model of a shear mode type MR damper [41].

active device in a few milliseconds. Its characteristics are summarized: (1) an MR damper is operated with low power sources, e.g., SD-1000 MR damper can generate a force up to 3000 N using a small battery with capacity less than 10 W; (2) it has high yield stress level, e.g., its maximum yield stress is beyond 80 kPa; (3) the performance is stable in broad temperature range, e.g., MR fluids operate at the temperature between –40 and 150°C; (4) the response time is a few milliseconds; (5) the performance is not sensitive to contamination during manufacturing of the MR damper. Moreover, the operating point of the MR damper, which is a current-controlled device, can be changed by a permanent magnet [33].

Adequate modeling of the control device is essential for accurately predicting the behavior of the controlled system. A number of mechanical models for non-linear damper system have recently been proposed by several researchers [12, 53, 54]. In this paper, a simple mechanical model consist of a Bouc-Wen element in parallel with a viscous damper is used, as shown in Fig. 6. This model has been verified to predict accurately the behavior of a prototype shear-mode MR damper over a wide range of inputs in a set of experiments [20, 21], and is also expected to be appropriate to model a full-scale MR damper [23].

The equations governing the force f exerted by this model are as follows [41]:

$$f = c_0\dot{x} + \alpha z \qquad (14)$$

$$\dot{z} = -\gamma|\dot{x}|z|\dot{z}|^{n-1} - \beta\dot{x}|z|^n + A_m\dot{x} \qquad (15)$$

Table 2. Parameters of the MR damper model.

α_a (N/cm)	1.0872×10^5
α_b (N/cm.V)	4.9616×10^5
c_{0a} (N.s/cm)	4.40
c_{0b} (N.s/cm.V)	44.0
A_m	1.2
n	1
β (1/cm)	3
γ (1/cm)	3
η (1/s)	50

where x is the displacement of the device, z is the evolutionary variable that accounts for the history dependence of the response. The parameters γ, β, n, and A_m are adjusted to determine the linearity in the unloading and the smoothness of the transition from the pre-yield region to the post-yield region. Device model parameters α and c_o are determined by the dependency on the control voltage u_c, as follows:

$$\alpha = \alpha(u) = \alpha_a + \alpha_b u_c \tag{16}$$

$$c_0 = c_0(u) = c_{0a} + c_{0b} u_c . \tag{17}$$

Therefore, the control voltage applied to the current driver in the MR damper continuously modulates the damping force of the MR damper. Moreover, to account for a time-lag in the response of the device to the changes in the command input, the first-order filter dynamics are introduced into the system as follows:

$$\dot{u} = -\eta(u_c - \upsilon) \tag{18}$$

where υ is command voltage applied to the control circuit, and η is the time constant of the first-order filter.

In order to obtain a dynamic model of an MR damper with a capacity of 1000 kN, the parameters of a shear-mode prototype MR damper were identified from the test results obtained at Washington University, and scaled up so as to have the maximum capacity of 1000 kN with the maximum command voltage $V_{max} = 10$ V [23]. These parameters are listed in Table 2 [41].

The hysteretic behavior of the MR damper model according to the input voltage is shown in Fig. 7.

Installation layout of MR dampers are illustrated in Fig. 8. The MR dampers are attached to the platform in diagonal fashion. The effectiveness of installation layout of MR dampers on offshore steel jacket platform has been verified in Ref. [44]. In what follows, a methodology which designs a control law for operation of an MR damper is addressed.

4.2 Motion equations of intelligent offshore structure

The jacket-type offshore structure is modeled using 12 nodes and 21 general beam elements. The dynamical differen-
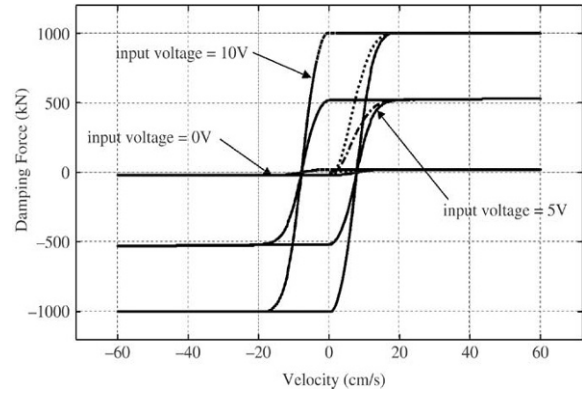

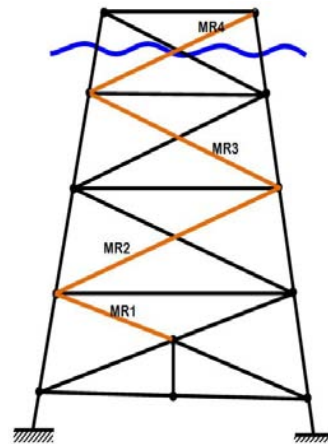Fig. 7. Hysteretic behavior of an MR damper [41].

Fig. 8. Installation layout of MR dampers on offshore platform [44].

tial equation of motion of semi-actively controlled 30-DOFs structural system subjected to external wave loads and control forces can be expressed as:

$$M\ddot{x} + C_d \dot{x} + Kx = \Gamma f_w + \Lambda f_{MR} \tag{19}$$

where $\mathbf{M}$, $\mathbf{C}_d$, and $\mathbf{K}$ are 30×30 mass, damping, and stiffness matrices of structure, respectively, $\mathbf{\Gamma}$ is 30×30 location matrix for hydrodynamic wave force vector $\mathbf{f}_w$, $\mathbf{f}_w$ is 30×1 wave force vector acting on nodes 3-12 of offshore structure, $\mathbf{\Lambda}$ is 30×4 location matrix for forces produced by MR dampers $\mathbf{f}_{MR}$, $\mathbf{f}_{MR}$ is 4×1 vector for forces produced by MR dampers 1-4 through clipped optimal control algorithm, $\ddot{\mathbf{x}}$, $\dot{\mathbf{x}}$ and $\mathbf{x}$ are 30×1 the acceleration, the velocity and the displacement vectors of the structure nodes relative to the ground, respectively.

Rayleigh's technique is used to estimate damping in the structure [48]. In this technique, it is assumed that the damping matrix $\mathbf{C}_d$ is proportional to the mass matrix $\mathbf{M}$ and the stiffness matrix $\mathbf{K}$, or:

$$C_d = \alpha M + \beta K \tag{20}$$

where α and β are related somehow to the critical damping of first two modes of vibration [48]. The values of α and β are

determined by Eqs. (21) and (22).

$$\alpha = 2\zeta \frac{\omega_1 \omega_2}{\omega_1 + \omega_2} \tag{21}$$

$$\beta = 2\zeta \frac{1}{\omega_1 + \omega_2}. \tag{22}$$

Eq. (19) can be written in the state-space form as:

$$\begin{cases} \dot{z} = Az + Bf_{MR} + Gf_w \\ y = Cz + Df_{MR} \end{cases} \tag{23}$$

where:

$$z = \begin{bmatrix} x \\ \dot{x} \end{bmatrix} \tag{24}$$

$$x = [U_3 \quad V_3 \quad \theta_{z3} \quad . \quad . \quad . \quad U_{12} \quad V_{12} \quad \theta_{z12}]^T \tag{25}$$

$$A = \begin{bmatrix} 0_{30\times30} & I_{30\times30} \\ -M^{-1}K & -M^{-1}C_d \end{bmatrix} \tag{26}$$

$$B = \begin{bmatrix} 0_{30\times30} \\ M^{-1}\Lambda \end{bmatrix} \tag{27}$$

$$G = \begin{bmatrix} 0_{30\times4} \\ M^{-1}\Gamma \end{bmatrix} \tag{28}$$

$$D = 0 \tag{29}$$

where z is the state space vector, y is output vector, A is state matrix, B is control input matrix, G is disturbance input matrix, C is output matrix, U_i and V_i are nodal displacements along X and Y-axis, respectively, and θ_{zi} is rotation about Z-axis, $i = 3, ..., 12$.

It should be noted that to measure the feedback signal to the semi-active controller, four accelerometers and four displacement transducers are used. All of the accelerometers and displacement transducers are positioned on nodes 9-12 so as to measure the velocity and the displacement of these structural nodes along X-axis.

5. Clipped optimal control algorithm

Generally, an MR damper cannot be directly controlled by a control algorithm. The reason is that a controller generates force signals while the MR damper requires voltage or current signals to be operated. Therefore, there are two solutions to this problem: (1) to use an inverse MR damper model, (2) to implement a converting algorithm. Candidates for the inverse MR damper models may include Bingham, Bouc-Wen, and modified Bouc-Wen models. Another good candidate for conversion is clipped algorithm.

The clipped optimal control strategy for an MR damper usually involves two steps. The first step is to assume an ideal actively–controlled device and construct an optimal controller for this active device. This optimal active controller is designed as the primary controller. The primary controller determines the ideal optimal force required for the MR damper. However, the dissipative property that is inherent in the semi-active device does not guarantee that the desired optimal force will coincide with the actual damping force. In the second step, a secondary controller finally determines the input voltage of the MR damper, so that the actual damping force approximately tracks the desired force commanded by the primary controller. That is, the secondary controller clips the optimal force in a manner consistent with the dissipative nature of the devise.

The clipped optimal control approach is to append a force feedback loop to induce the MR damper, to produce approximately a desired control force f_c. The linear quadratic regulator algorithm has been employed both for active control [55] and for semi-active control [56]. Using this algorithm, the optimal control force f_c for f, which is force generated by a MR damper, may be obtained by minimizing the following scalar performance index.

$$J = \int_{t_0}^{t_f} (x^T Q x + f_c^T R f_c) dt \tag{30}$$

The time interval $[t_0, t_f]$ in the integral Eq. (30) is defined to be longer that of the external excitation. Also, **Q** is a $2N \times 2N$ positive semi-definite matrices (**Q** ≥ 0), and **R** is an $m \times m$ positive definite matrix (**R** > 0).

Q and **R** are weighting matrices and their values are selected depending on the relative importance given to different terms in their contributions to the performance index J. Large values of **Q** represent the desire of keeping the state vector close to the origin during the minimization interval $[t_0, t_f]$, whilst large values of **R** imply a moderate level of control.

Solving the optimal control problem with J defined by Eq. (30), results in a optimal force vector $\mathbf{f}_c$ regulated only by the state vector $\mathbf{x}$, such that

$$f_c = -R^{-1}B^T P x = -K_{lqr} x \tag{31}$$

where matrix $\mathbf{K}_{lqr}$ represents the LQR optimal gain matrix, and the matrix **P** is the solution of the classical Riccati equation given by:

$$PA + A^T P - PBR^{-1}B^T P + Q = 0. \tag{32}$$

It should be noted that in Eq. (31), the feedback is of the full state **x** of the system. However, in a practical situation it is not always possible to obtain the entire states of the system, due to noise existence and etc., and often the output is a possible combination of all the states.

When there are process noise, as disturbance, and measurement noise, as sensor noise, Eq. (18) is changed to:

$$\begin{cases} \dot{z} = Az + Bf_{MR} + Gf_w + \varepsilon_1 \\ y = Cz + Df_{MR} + \varepsilon_2. \end{cases} \tag{33}$$

The vectors ε_1 and ε_2 in Eq. (33) represent the process noise and the measurement noise, respectively. They are assumed as zero-mean Gaussian white noise, satisfying the following equation:

$$E[\varepsilon_1\varepsilon_1^T] = Q_e\delta(t-\tau) \qquad Q_e = Q_e^T \qquad (34)$$

$$E[\varepsilon_2\varepsilon_2^T] = R_e\delta(t-\tau) \qquad R_e = R_e^T \qquad (35)$$

$$E[\varepsilon_1\varepsilon_2^T] = 0 \qquad (36)$$

where $\mathbf{Q}_e$ and $\mathbf{R}_e$ are semi-definite and definite matrices, respectively, $\delta(t)$ is Dirac function.

When the full state is not available, the state $\mathbf{x}$ is replaced in Eq. (31) by an optimal state estimate $\hat{\mathbf{x}}$ generated by a Kalman filter which is given by:

$$\begin{cases} \dot{\hat{x}} = (A - BK_{lqr} - K_eC)\hat{x} + K_{es}y \\ \hat{y} = C\hat{x} \end{cases} \qquad (37)$$

where $\hat{\mathbf{x}}$ is the state estimate to $\mathbf{x}$, $\mathbf{K}_{es}$ is the gain of the Kalman filter is given by:

$$K_{es} = P_eC^TR^{-1}. \qquad (38)$$

In which $\mathbf{P}_e$ is the stabilizing solution to the Riccati equation:

$$P_eA + A^TP_e - P_eBR_e^{-1}B^TP_e + Q_e = 0 \qquad (39)$$

so Eq. (31) is changed to:

$$f_c = -R^{-1}B^TP\hat{x} = -K_{lqr}\hat{x}. \qquad (40)$$

The force generated by the MR damper cannot be commanded; only the voltage v applied to the current driver for the MR damper can be directly changed. To induce the MR damper to generate approximately the desired optimal control force f_c, the command signal v is selected as follows. When the MR damper is providing the desired optimal force (i.e., $f = f_c$), the voltage applied to the damper should remain at the present level. If the magnitude of the force produced by the damper is smaller than the magnitude of the desired optimal force and the two forces have the same sign, the voltage applied to the current driver [23] varies continuously in the range of [0-V_{max}]. The secondary controller for continuously varying the command voltage can be stated as:

$$v_i = V_{ci}H(\{f_{ci} - f_i\}f_i) \qquad (41)$$

$$V_{ci} = \begin{cases} \mu_if_{ci} & , \quad for \quad f_{ci} \leq f_{max} \\ V_{max} & , \quad for \quad f_{ci} > f_{max} \end{cases} \qquad (42)$$

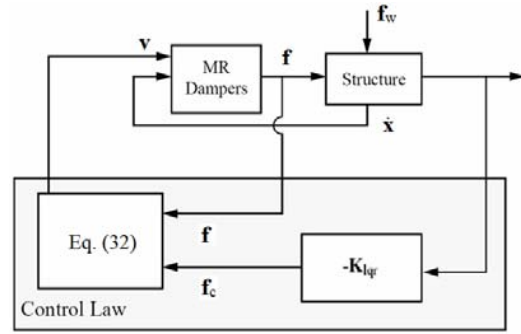where f_{max} is maximum force produced by the damper (=1,000

Fig. 9. Semi-active strategy using clipped optimal algorithm.

kN), μ is coefficient relating the voltage to the force (=V_{max}/f_{max}), $H(.)$ is the Heaviside step function expressed as 0 or 1 [23], f_i is the force produced by i^{th} MR dampers which is applied to the structure. The block diagram of clipped optimal control algorithm is shown in Fig. 9.

6. Neuro-fuzzy control strategy

The idea of the proposed control strategy is to replace the traditional semi-active control strategy, clipped optimal control algorithm, for MR dampers with an intelligent control scheme which is trained by collected time histories of offshore steel jacket platform response and voltage produced by clipped optimal control system during applying wave-induced forces. In the proposed control algorithm, there is no need to calculate MR damper forces by solving a set of differential equation which is computationally expensive. Moreover, the speed of execution of this algorithm is higher than the model-based controllers. Another important characteristic of this control scheme is its robustness which is especially desirable in structural control applications characterized by uncertainties.

In this research, vibration of offshore structure due to wave forces is controlled by use of clipped optimal control algorithm with LQR target controller at first. The data obtained by this algorithm is used to train different parts of proposed neuro-fuzzy control scheme. Once trained, the clipped optimal control algorithm is automatically removed from the control loop and the neuro-fuzzy control algorithm takes on. In case of a change in the parameters of the system under control, the clipped optimal control algorithm with LQR controller enters the control loop again and different parts of proposed control strategy gets trained again for the new condition. The architecture of this strategy is shown in Fig. 10.

This architecture consists of four parts to perform different tasks. The first part is the dynamic-feedback neural network to be trained on-line in order to generate the one step ahead prediction of displacement and velocity of connected nodes to MR dampers along X-axis (U_{ik+1}, U_{jk+1}, $\dot{U}_{ik+1}$, $\dot{U}_{jk+1}$). Inputs to this network are the delayed outputs (U_{ik-2}, U_{ik-1}, U_{ik}, $\dot{U}_{jk-2}$, $\dot{U}_{jk-1}$, $\dot{U}_{jk}$), the delayed MR damper forces (f_{MRk-2}, f_{MRk-1}, f_{MRk}), the delayed wave-induced forces applied to connected nodes to MR dampers along X-axis (f_{wxik-2}, f_{wxik-1}, f_{wxik}, f_{wxjk-2}, f_{wxjk-1}, f_{wxjk})
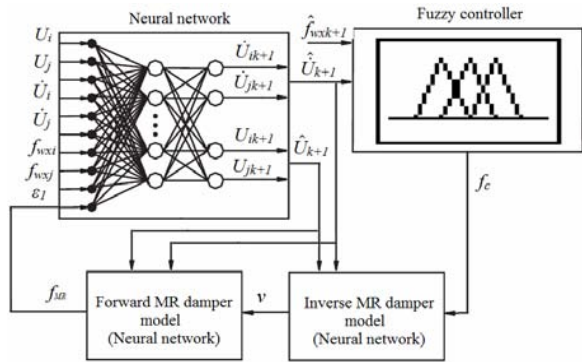
Fig. 10. Architecture of the neuro-fuzzy control strategy.

and the delayed process noise (ε_{1k-2}, ε_{1k-1}, ε_{1k}). At the initial time, the delayed inputs of the network will be taken to have the value of zero in accordance with the actual initial circumstance. The second part is the fuzzy controller, whose inputs are the relative wave-induced force applied along MR damper $\hat{f}_{wxk+1}$ and the velocity of MR damper $\hat{U}_{k+1}$. The output of the fuzzy controller is desired control force of the MR damper f_c. The aim of this part is to determine desired control forces of the MR dampers quickly in accordance with the relative wave-induced forces applied along MR dampers $\hat{f}_{wxk+1}$ and the velocities of MR dampers $\hat{U}_{k+1}$. How to design the fuzzy controller and determine the desired control forces of MR dampers will be detailed in the following section. The third part is the feedforward neural network to be trained on-line to generate the required voltage of MR damper v. In fact, this part is the inverse dynamics model of MR damper. Unfortunately, due to the inherent non-linear nature of the MR damper, a model for inverse dynamics of MR damper is difficult to obtain mathematically. Because of this reason, a feedforward back propagation neural network is constructed to copy the inverse dynamics of the MR damper. This neural network model is trained using input-output data generated analytically using the simulated MR model based on Eqs. (14)-(18), (41) and (42). Using this inverse dynamics of MR damper, the required voltage signal v is calculated based on the desired control force f_c, the velocity of MR damper $\hat{U}_{k+1}$, and the displacement of MR damper $\hat{U}_{k+1}$. The fourth part is the feedforward back propagation neural network to be trained on-line in order to generate the MR damper forces f_{MR}. The inputs of this neural network are voltage signal v, the velocity of MR damper $\hat{U}_{k+1}$, and the displacement of MR damper $\hat{U}_{k+1}$.

6.1 The neural network based on Levenberg Marquardt algorithm

Neural network is a simplified model of the biological structure found in human brains. This model consists of elementary processing units (also called neurons). It is the large amount of interconnections between these neurons and their capability to learn from data to enable neural network as a strong predicting and classification tool. In this study, a three-layer dynamic-feedback neural network, which consists of an input layer, a hidden layer and an output layer, is selected for the first part of neuro-fuzzy control system to predict the responses of offshore steel jacket platform with MR dampers subjected to wave-induced forces. In this neural network, input layer with 24 nodes, hidden layer with 10 nodes and output layer with 4 nodes were adopted as one of the best suitable topologies. The most suitable input data for this study was found to be the current and two previous histories for displacement and velocity of connected nodes to MR dampers along X-axis, MR damper forces, wave-induced forces applied to connected nodes to MR dampers along X- axis, and process noise. The third and fourth part of the proposed neuro-fuzzy control strategy which is a three-layer feedforward neural network consists of an input layer with 3 nodes, a hidden layer with 20 nodes, and output layer with one node. Determining the numbers of inputs, outputs, hidden layers and nodes in hidden layers of these three neural networks is done by trial and error.

The net input value net_k of the neuron k in some layer and the output value O_k of the same neuron can be calculated by the following equations:

$$net_k = \sum w_{jk} O_j \tag{43}$$
$$O_k = f(net_k + \theta_k) \tag{44}$$

where w_{jk} is the weight between the jth neuron in the previous layer and the kth neuron in the current layer, O_j is the output of the jth neuron in the previous layer, $f(.)$ is the neuron's activation function which can be a linear function, a radial basis function, and a sigmoid function, and θ_k is the bias of the kth neuron.

Feedforward neural network often has one or more hidden layers of tangent sigmoid neurons followed by an output layer of linear neurons. Multiple layers of neurons with non-linear transfer functions allow the network to learn non-linear and linear relationships between input and output vectors. In the neural network parts of proposed neuro-fuzzy control strategy, the tangent sigmoid transfer function is chosen as the activation function of the hidden layer:

$$O_k = f(net_k + \theta_k) = \frac{1 + e^{-2(net_k + \theta_k)}}{1 + e^{-2(net_k + \theta_k)}}. \tag{45}$$

The linear transfer function is chosen as the activation function of the output layer:

$$O_k = f(net_k + \theta_k) = net_k + \theta_k. \tag{46}$$

It should be noted that neural network parts need to be trained before doing their different tasks. As the inputs are applied to the neural networks, the network outputs are compared with the targets. The difference or error between both is processed back through the network to update the weights and biases of the neural network so that the network outputs match

closer with the targets. The input and output data are usually represented by vectors called training pairs. The process as mentioned above is repeated for all the training pairs in the data set, until the network error converged to a threshold minimum defined by a corresponding performance function. In this paper, the Mean Square Error (MSE) function is adopted. The desired MSE for the networks is 1e-7.

Levenberg-Marquardt (LM) algorithm [57] is adopted to train the neural network parts, which can be written as

$$w^{i+1} = w^i - \left[\frac{\partial^2 E}{\partial w^{i^2}} + \mu I \right]^{-1} \frac{\partial E}{\partial w^i} \tag{47}$$

where i is the iteration index, $\partial E / \partial w^i$ is the gradient descent of the performance function E with respect to the parameter matrix w^i, $\mu \geq 0$ is the learning factor, and I is the unity matrix.

During the vibration process, the neural network updates the weights and bias of neurons real time in accordance with sampling pairs till the objective error is satisfied, i.e. the property of the structure is acquired. As we know, the main aim of the first neural network is to predict the dynamic responses of the offshore structure, and to provide inputs of the fuzzy controller and data of calculating control force of MR dampers. Thus outputs of the neural network are displacement and velocity of connected nodes to MR dampers along X-axis (U_{ik+1}, U_{jk+1}, $\dot{U}_{ik+1}$, $\dot{U}_{jk+1}$). In order to predict the dynamic responses of offshore structure, required voltage of MR dampers, and forces of MR dampers, the most direct and important factors which affect the predicted results are considered.

6.2 Design of fuzzy controller

In 1985, Takagi and Sugeno [58] suggested an effective way for modeling of complex non-linear dynamic systems by introducing linear equations in consequent parts of a fuzzy model, which is called Takagi-Sugeno fuzzy model. It has led to reduction of computational cost because it does not need any defuzzification procedure.

The fuzzy model proposed in this research is based on a first order Takagi-Sugeno-Kang (TSK) architecture that is generally composed of r rules of the form

Rule i: IF x_1 is A_{11} and x_2 is A_{i2}…and x_n is A_{in}
     THEN $y = b_{io} + b_{i1}x_1 + b_{i2}x_2 + … + b_{in}x_n$

where x_1, x_2, …, x_n are antecedent variables, and y is the consequent variable. A_{11}, A_{i2}, …, and A_{in} are fuzzy sets defined over the domains of the respective antecedents. b_{io}, b_{i1}, …, b_{in} are constant coefficients that characterize the linear relationship defined by the ith rule in the rule set, $i = 1, 2, …, r$. A TSK fuzzy model is computationally efficient platform that is well suited for implementation of non-linear associations through the construction of many piecewise linear relationships [59]. The need to approximate such a function is obvious given the
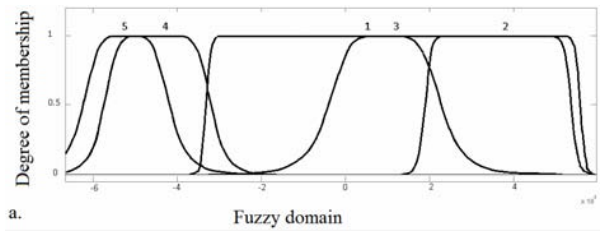

Fig. 11. The membership function curves of the relative wave-induced force applied along MR damper 1.
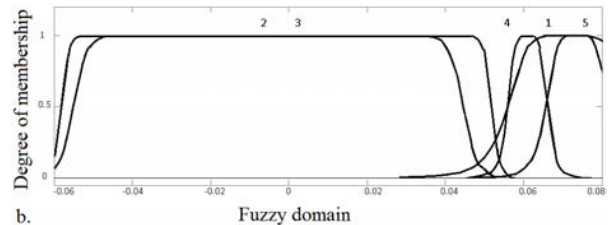

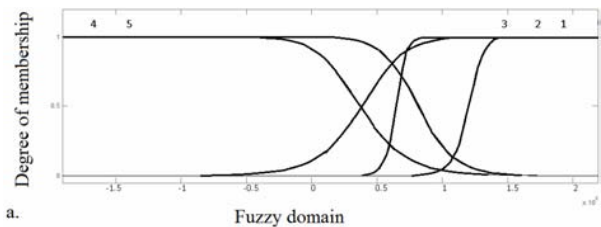Fig. 12. The membership function curves of the velocity of MR damper 1.

Fig. 13. The membership function curves of the relative wave-induced force applied along MR damper 2.

non-linear nature of an MR damper.

The first step of designing fuzzy controller is determining the basic domains of inputs and outputs. Relative wave-induced force applied along MR damper $\hat{f}_{wxk+1}$ and the velocity of MR damper $\hat{U}_{k+1}$ are chosen as inputs of the fuzzy controller, because considered input influence the desired control forces of MR dampers directly. The domain of relative wave-induced force applied along MR damper and velocity of MR damper is determined in accordance with their amplitude which has been obtained from clipped optimal control algorithm.

The membership functions are usually chosen in accordance with the characters of the membership functions and designing experience. In this paper, bell shape membership function is adopted as the membership functions of relative wave-induced force applied along MR damper $\hat{f}_{wxk+1}$ and the velocity of MR damper $\hat{U}_{k+1}$. The selection of bell shape membership functions for fuzzy inputs is for their best performance in comparison with other kind of membership functions. This has been obtained by trial and error. The membership function curves of relative wave-induced force applied along MR damper and the velocity of MR damper for MR dampers 1-4 are plotted in Figs. 11-18.

Fig. 14. The membership function curves of the velocity of MR damper 2.

Fig. 15. The membership function curves of the relative wave-induced force applied along MR damper 3.

Fig. 16. The membership function curves of the velocity of MR damper 3.

Fig. 17. The membership function curves of the relative wave-induced force applied along MR damper 4.

Fig. 18. The membership function curves of the velocity of MR damper 4.

Table 3. Hydrodynamic specifications.

H (m)	4.92
T (s)	8.71
λ (m)	116.94
ρ_w (kg/m³)	1027
ψ (°)	135
C_D	1.2
C_M	2
ω (rad/s)	0.72

7. Numerical example

To evaluate the neuro-fuzzy control strategy for the offshore steel jacket platform with MR dampers, a numerical example is considered in which a model of offshore steel jacket platform is controlled with four MR dampers, as shown in Fig. 8. The offshore structure consists of the cylindrical steel members. The Young's modulus of steel members E is 200 GPa. The density of steel ρ is 7860 kg/m³. Geometric properties of cylindrical members of the offshore platform under study are given in Table 1. The hydrodynamic specifications can be found in Table 3 [50]. Using these data, the wave-induced forces can be calculated from Eq. (13) with the water depth $d = 47$ m. in Table 3, ψ is the angle of wave incidence.

For simplicity of presentation, only the first two modes of vibration are considered because these two modes are the most dominant and hence the most important for the design of the control system. The natural frequencies of the first two modes of vibrations are such that $\omega_1 = 1.0037 \times 10^3$ rad/sec and $\omega_2 = 4.8131 \times 10^3$ rad/sec. The structural damping in each mode is considered to be 1%, hence $\zeta_1 = \zeta_2 = 0.01$. Damping of the structure is obtained using Eq. (20). Matrices $\mathbf{Q}$, $\mathbf{R}$, $\mathbf{Q}_e$, and $\mathbf{R}_e$ are defined below:

$$R = 10^{-6} I_{4\times4} \qquad (48)$$

$$Q = 10^{10} diag(1,0,0,1,0,0,1,0,0,1,0,0,1,0,0, \\ 1,0,0,1,0,0,1,0,0,1,0,0,1,0,0, zeros(1,30)) \qquad (49)$$

$$Q_e = 9.83 \times 10^{-5} I_{35\times35} \qquad (50)$$

$$R_e = 2.45 \times 10^{-7} I_{60\times60}. \qquad (51)$$

In the example, the model of the offshore structure is subjected to wave-induced forces, and the sampling time is 0.001 s. Some programs about the neuro-fuzzy control strategy on the offshore structure with MR dampers are made in Matlab language.

As mentioned previously, the horizontal displacement of the offshore structures needs to be limited to ensure safety. Moreover, horizontal acceleration also needs to be restricted for the comfort of people who work on the offshore platforms. Therefore, the control objective is to reduce both the peak displacement and acceleration responses of the offshore steel
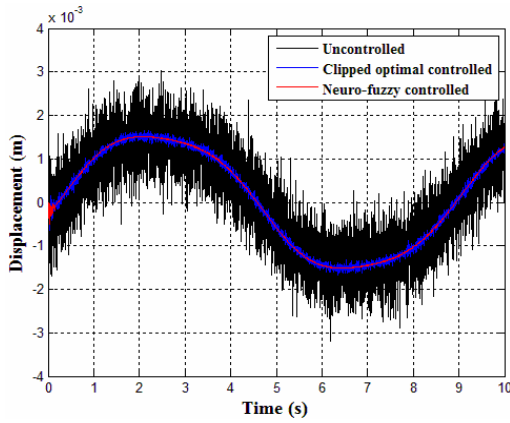
Fig. 19. The time history of displacement responses of node 4.
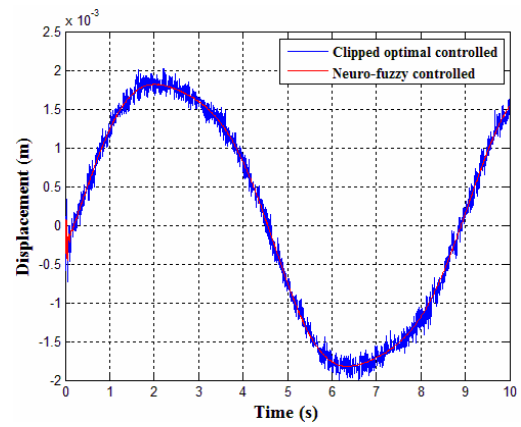

Fig. 22. The time history of displacement responses of node 6.
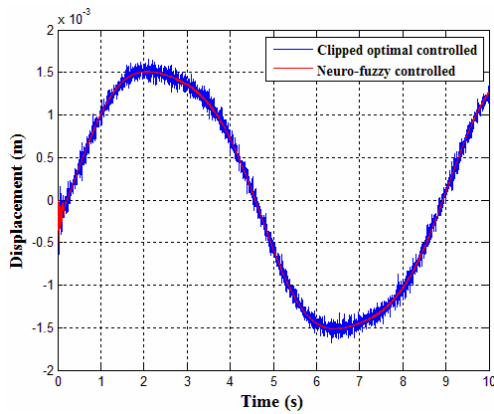

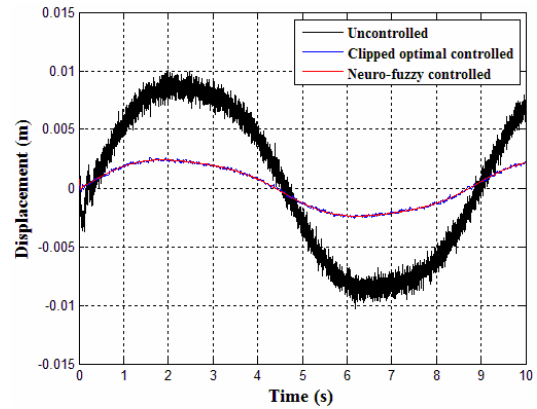Fig. 20. The time history of displacement responses of node 4.

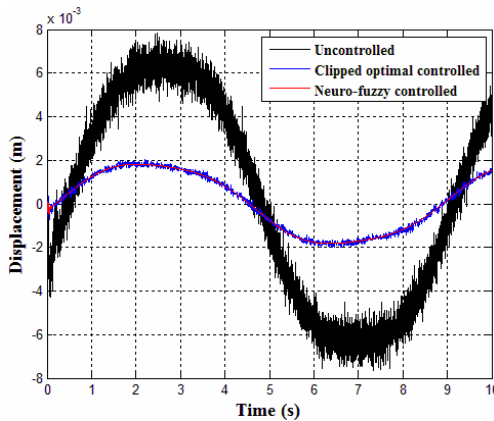Fig. 23. The time history of displacement responses of node 7.

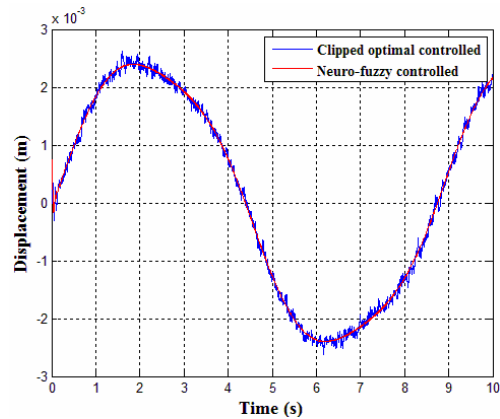Fig. 21. The time history of displacement responses of node 6.

Fig. 24. The time history of displacement responses of node 7.

jacket platforms. The responses of the offshore steel jacket platform with the MR dampers controlled by the neuro-fuzzy control strategy are compared with the responses of the off-shore steel jacket platform without the MR dampers and the offshore steel jacket platform with the MR dampers controlled by clipped optimal control strategy with LQG-target controller, while the system is distributed by zero-mean Gaussian white noise. Comparisons between neuro-fuzzy controlled, clipped

optimal controlled with LQG-target controller, and uncontrolled system are evaluated in terms of displacement and acceleration responses of nodes 4, 6, 7, 10, and 11 along X-axis. The displacement responses comparison between the neuro-fuzzy controlled, clipped optimal controlled with LQG-target controller, and uncontrolled offshore structure are shown in Figs. 19-28. Note that, the system is distributed by process/sensing noise from a zero-mean Gaussian white noise
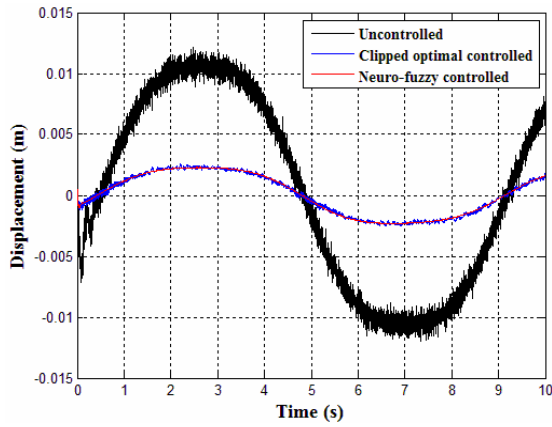
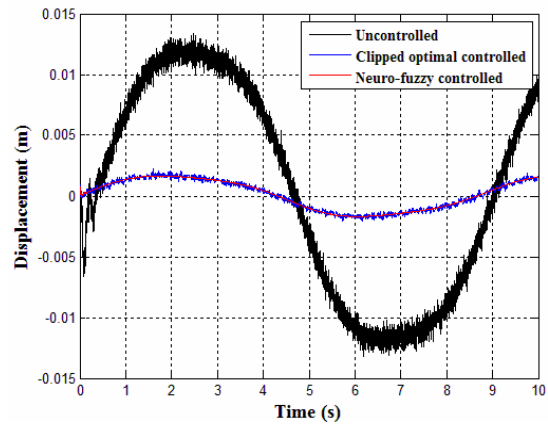Fig. 25. The time history of displacement responses of node 10.

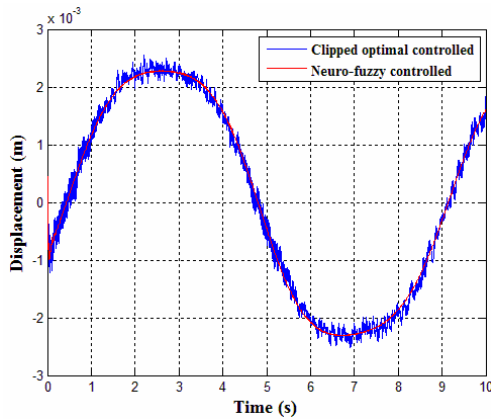Fig. 27. The time history of displacement responses of node 11

Fig. 26. The time history of displacement responses of node 10.
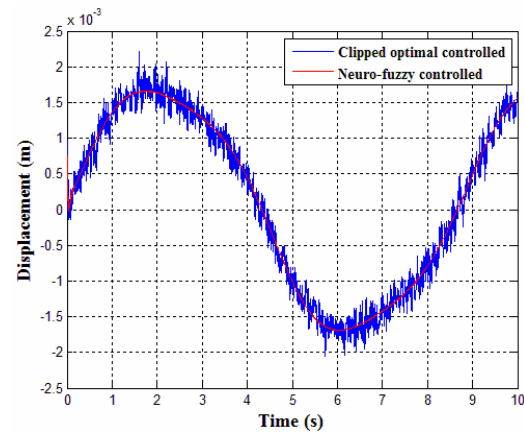

Fig. 28. The time history of displacement responses of node 11.

generator.

Figs. 19-28 show that both the clipped optimal with LQG-target controller and the neuro-fuzzy control systems are effective in reducing the wave-induced vibration of offshore steel jacket platform with severe process/sensing noises. However, the neuro-fuzzy control system yields smaller displacement responses than the clipped optimal control system with LQG-target controller. In addition, the neuro-fuzzy control system is more robust to process/sensing noises than the clipped optimal control system with LQG-target controller. As mentioned, the robustness of the proposed control systems is due to its soft computing components, i.e. first neural network part. Moreover, the speed of execution of this algorithm is higher than that of the clipped optimal control scheme with LQG target controller.

The time history of acceleration responses of the uncontrolled, clipped optimal controlled with LQG-target controller and neuro-fuzzy controlled offshore structure with process/sensing noises are shown in Figs. 29-33. Transient acceleration response of nodes 4, 6, 7, 10, and 11 in the first two seconds have been omitted to show the steady-state acceleration response.

According to the Figs. 29-33 the control effect of the neuro-fuzzy control strategy is better than that of the clipped optimal control strategy with LQG-target controller for acceleration responses. Moreover, the neuro-fuzzy control system can handle the effect of process/sensing noises better than that of the clipped optimal control system with LQG-target controller. The most important conclusion is that use of the proposed neuro-fuzzy control strategy makes the situation of people on the platform more comfortable. Based on the simulation results, it can be concluded that the control strategy is very important for semi-active control. The voltage signals used for training of the inverse dynamics of MR dampers 1-4, i.e. target voltage signals obtained by clipped optimal control algorithm, are compared with the voltage signals obtained by inverse dynamic of MR dampers 1-4, i.e. neural network prediction, in Figs. 34-37, respectively.

Similarities between the above two voltage signals show that even though determination of the control signal, i.e. voltage signal, from the target controller is based on displacement and velocity of the offshore structure, a strong correlation exists between inputs of the neural network and the voltage signal.
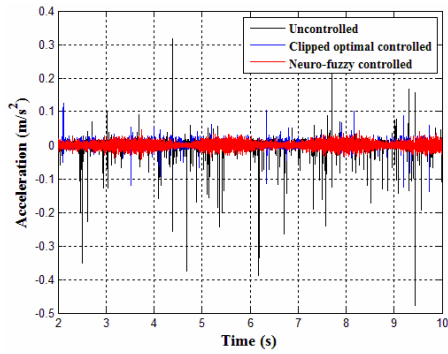
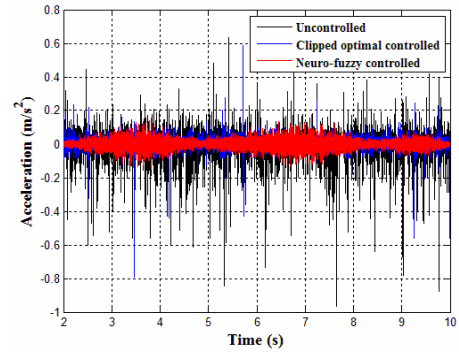Fig. 29. The time history of acceleration responses of node 4.

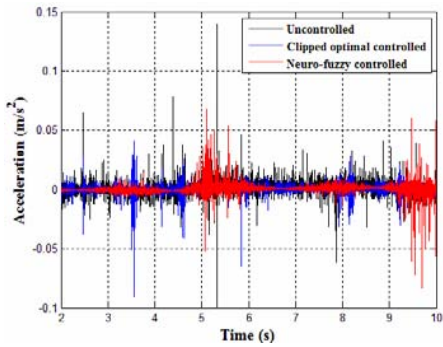Fig. 30. The time history of acceleration responses of node 6.

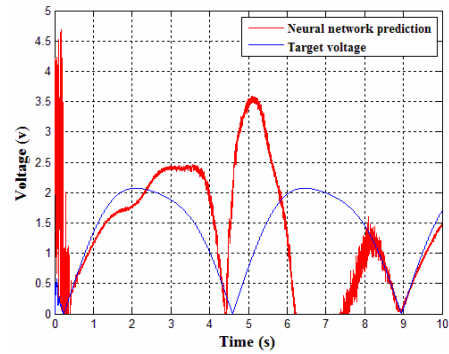Fig. 31. The time history of acceleration responses of node 7.

Fig. 32. The time history of acceleration responses of node 10.

Fig. 33. The time history of acceleration responses of node 11.

Fig. 34. Comparison of target voltage and voltage predicted by inverse dynamics of MR damper 1.
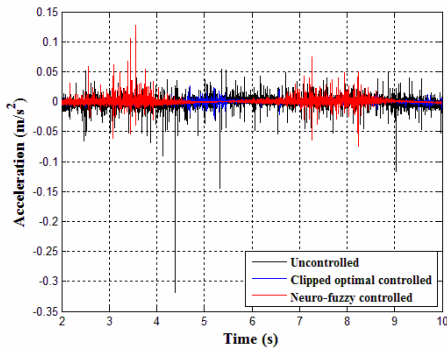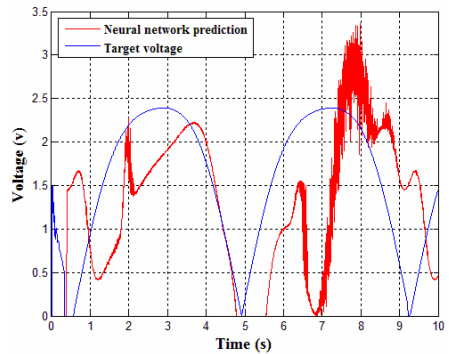

Fig. 35. Comparison of target voltage and voltage predicted by inverse dynamics of MR damper 2.

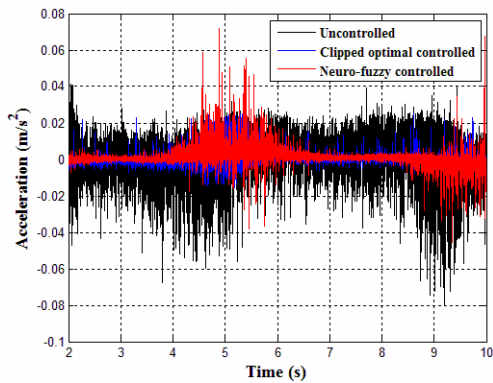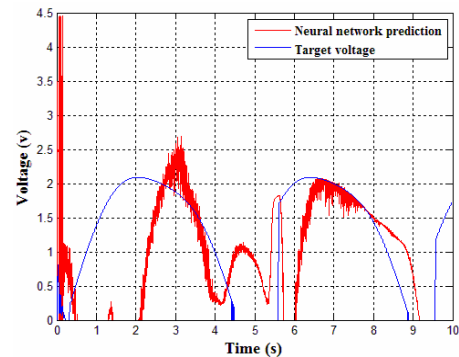

Fig. 36. Comparison of target voltage and voltage predicted by inverse dynamics of MR damper 3.
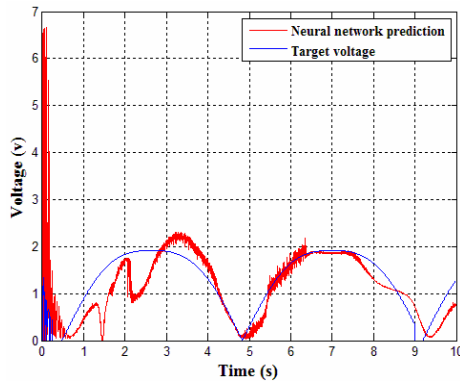
Fig. 37. Comparison of target voltage and voltage predicted by inverse dynamics of MR damper 4.

8. Conclusions

In this paper, a neuro-fuzzy control strategy is proposed for control of wave-induced vibration of an offshore steel jacket platform equipped with MR dampers. Practical benefits of the proposed control scheme are numerous. The most important characteristic of the proposed intelligent control strategy is its inherent robustness and its ability to handle the non-linear behavior of the system. Besides, no mathematical model is needed to calculate forces produced by MR dampers, and the speed of execution of this algorithm is higher than the model-based controllers. Wave-induced forces are determined according to linearized Morison equation. The performance of the proposed neuro-fuzzy control system is compared with that of a traditional semi-active control strategy, i.e., clipped optimal control system with LQG-target controller, through computer simulations, while the uncontrolled system response is used as the baseline. It is demonstrated that the proposed control system design framework is more effective than that of the clipped optimal control scheme with LQG-target controller to reduce the vibration of offshore structure. Furthermore, the neuro-fuzzy control strategy is more robust to process/sensing noises than the clipped optimal control algorithm with LQG-target controller. It can be concluded that the control strategy is very important for semi-active control.

Acknowledgment

Nomenclature———————————————————————

A	: State matrix
A	: Cross sectional area of element
a	: Half of element length
A_m	: Constant parameter
B	: Control input matrix
C	: Output matrix

c	: Wave celerity
C_D	: Drag coefficient
C_d	: Damping matrix of offshore structure
C_M	: Inertia coefficient
c_o	: Constant parameter
d	: Water depth
dA	: Projected area of offshore structure member normal to member axis
df_w	: Wave force per unit length of offshore structure member
dV	: Displaced volume of offshore structure member normal to member axis
E	: Young's modulus of steel element
f	: Force vector exerted by MR damper model
f	: Force exerted by MR damper model
$f(.)$	: Neuron's activation function
f_c	: Control force vector produced by target controller
f_c	: Control force produced by target controller
F_e	: Force vector applied on structural element in global coordinate system
f_e	: Force vector applied on structural element in local coordinate system
f_i	: Force produced by i^{th} MR damper
f_{MR}	: Force vector produced by MR dampers
f_{max}	: Maximum force produced by MR damper
f_w	: Wave force vector
f_{xi}	: Force applied on node i in x direction
f_{yi}	: Force applied on node i in y direction
$\hat{f}_{wxk+1}$	: Relative wave-induced force applied along MR damper
j	: Performance index
H	: Wave height
$H(.)$	: Heaviside step function
G	: Disturbance input matrix
I	: Unity matrix
i	: Iteration index
I_z	: Moment of inertia of cross section of beam element with respect to z-axis
K	: Stiffness matrix of offshore structure
k	: Wave number
K_e	: Stiffness matrix of element in global coordinate system
k_e	: Stiffness matrix of element in local coordinate system
K_{es}	: Kalman filter gain matrix
K_{lqr}	: LQR optimal gain matrix
l_e	: Element length
M	: Mass matrix of offshore structure
M_e	: Mass matrix of element in global coordinate system
m_e	: Mass matrix of element in local coordinate system
M_i	: Moments applied on node i
n	: Constant parameter
net_k	: Net input value of neuron k
O_k	: Output value of neuron k
O_j	: Output of jth neuron in previous layer

P	: Solution of classical Riccati equation
P_e	: Stabilizing solution to Riccati equation
Q	: Weighted matrix
Q_e	: Covariance matrix of process noise
q_n	: Time independent velocity of fluid normal to member axis at joint n
$\dot{q}_n$	: Time independent acceleration of fluid normal to member axis at joint n
R	: Weighted matrix
R_e	: Covariance matrix of measurement noise
T	: Transformation matrix
T	: Wave period
t	: Time
U_i	: Nodal displacement along X-axis
$\hat{U}_{k+1}$	: Predicted displacement of MR damper
$\hat{\dot{U}}_{k+1}$	: Predicted velocity of MR damper
U_{ik+1}	: Predicted displacement of connected node to MR damper
U_{jk+1}	: Predicted displacement of connected node to MR damper
$\dot{U}_{ik+1}$	: Predicted velocity of connected node to MR damper
$\dot{U}_{jk+1}$	: Predicted velocity of connected node to MR damper
V_i	: Nodal displacement along Y-axis
u	: Horizontal water particle velocity
u_c	: Control voltage
$\dot{u}$	: Horizontal water particle acceleration
u_i	: Nodal displacement along x-axis
v	: Vertical water particle velocity
v	: Command voltage applied to control circuit
$\dot{v}$	: Vertical water particle acceleration
v_i	: Nodal displacement along y-axis
V_{max}	: Maximum command voltage
w_{jk}	: Weight between j^{th} neuron in the previous layer and k^{th} neuron in current layer
x	: Displacement vector of offshore structure nodes relative to ground
x	: Location of joint along x-axis with respect to fixed reference
x	: Displacement of MR damper
$\dot{x}$	: Velocity vector of offshore structure nodes relative to ground
$\ddot{x}$	: Acceleration vector of offshore structure nodes relative to ground
$\hat{x}$	: State vector estimated by Kalman filter
$\dot{x}_n$	: Absolute velocity of joint n
y	: Location of joint along y-axis with respect to fixed reference
z	: State space vector
z	: Evolutionary variable that accounts for history dependence of response
0	: Null matrix
θ_k	: Bias of kth neuron
θ_{zi}	: Nodal rotation about z-axis
α	: Angle between x-axis and X-axis
ρ	: Mass density of element

ρ_w	: Mass density of water
λ	: Wave length
ω	: Wave frequency
ω_1	: Natural frequency of first mode of vibration
ω_2	: Natural frequency of first mode of vibration
σ_{vr}	: Root mean squares values of relative velocity between water particles and structure at each joint
β	: Constant parameter
γ	: Constant parameter
η	: Time constant of first-order filter
Γ	: Location matrix for hydrodynamic wave force vector
Λ	: Location matrix for forces produced by MR dampers
ζ	: Damping ratio
θ_{zi}	: Nodal rotation about Z-axis
ε_1	: Process noise vector
ε_2	: Measurement noise vector
δ	: Dirac function
μ	: Coefficient relating the voltage to force
μ	: Learning factor
ψ	: Angle of wave incidence

References

[1] M. Abdel-Rohman, Structural control of a steel jacket platform, *Structural and Engineering Mechanics*, 4 (2) (1996) 125-138.

[2] J. Suhardjo and A. Kareem, Feedback-feedforward control of offshore platforms under random waves, *Earthquake Engineering and Structural Dynamics*, (30) (2001) 213-235.

[3] H. J. Li, S. Hu and C. Jakubiak, H₂ active vibration control for offshore platform subjected to wave loading, *Sound and Vibration* (263) (2003) 709-724.

[4] H. Ma, G. Tang and Y. Zhao, Feedforward and feedback optimal control for offshore structures subjected to irregular wave forces, *Ocean Engineering* (33) (2006) 1105-1117.

[5] K. C. Patil and R. S. Jangid, Passive control of offshore jacket platforms, *Ocean Engineering* (32) (2005) 1933-1949.

[6] X. Chen, L. Wang and J. Xu, TLD technique for reducing ice-induced vibration on platforms, *Cold Regions Engineering (ASCE)*, 13 (3) (1999) 139-152.

[7] Q. Jin, X. Li, N. Sun, J. Zhou and J. Guan, Experimental and numerical study on tuned liquid dampers for controlling earthquake response of jacket offshore platform, *Marine Structures* (20) (2007) 238-254.

[8] J. Ou, X. Long, Q. Li and Y. Xiao, Vibration control of steel jacket offshore platform structures with damping isolation systems, *Engineering Structures* (29) (2007) 1525-1538.

[9] H. J. Li, S. Wang and C. Ji, Semi-active control of wave-induced vibration for offshore platforms by use of MR damper, *China Ocean Engineering*, 16 (1) (2002) 33-40.

[10] S. J. Dyke, B. F. Spencer Jr, M. K. Sain and J. D. Carlson, Modeling and control of magnetorheological dampers for seismic response reduction, *Smart Materials and Structures*, 5 (5) (1996) 565-575.

[11] S. J. Dyke, B. F. Spencer Jr, M. K. Sain and J. D. Carlson,

Experimental study of MR dampers for seismic protection, *Smart Materials and Structures: Special Issue on Large Civil Structures*, 7 (5) (1998) 693-703.

[12] S. J. Dyke, B. F. Spencer Jr, M. K. Sain and J. D. Carlson, Phenomenological model for magnetorheological dampers, *Engineering Mechanics*, 123 (3) (1997) 230-238.

[13] B. F. Spencer Jr, E. A. Johnson and J. C. Ramallo, ''Smart'' isolation for seismic control, *JSME International Journal: Special Issue on Frontiers of Motion and Vibration Control*, Series C, 43 (3) (2000) 704-711.

[14] J. C. Ramallo, E. A. Johnson and B. F. Spencer Jr, ''Smart'' base isolation systems, *Engineering Mechanics*, 128 (10) (2002) 1088-1099.

[15] H. Yoshioka, J. C. Ramallo and B. F. Spencer Jr, ''Smart'' base isolation strategies employing magnetorheological dampers, *Engineering Mechanics*, 128 (5) (2002) 540-551.

[16] G. Yang, B. F. Spencer Jr, J. D. Carlson and M. K. Sain, Large-scale MR fluid dampers: modeling and dynamic performance considerations, *Engineering Structures*, 24 (3) (2002) 309-323.

[17] H. Jung, H. Lee and W. H. Yoon, Semi-active neuron-control for seismic response reduction using smart damping strategy, *Computing in Civil Engineering (ASCE)*, 18 (3) (2004) 277-280.

[18] S. J. Dyke, B. F. Spencer Jr, M. K. Sain and J. D. Carlson, Seismic response reduction using magnetorheological dampers, *Proc. of IFAC World Congress* (1996).

[19] S. J. Dyke and B. F. Spencer, Seismic response control using multiple MR dampers, *Proc. of the 2nd International Workshop on Structural Control* (1996) 163-173.

[20] L. M. Jansen and S. J. Dyke, Semi-active control strategies for MR dampers: Comparative study, *Engineering Mechanics*, 126 (8) (2000) 795-803.

[21] F. Yi, S. J. Dyke, J. M. Caicedo and J. D. Carlson, Experimental verification of multi-input seismic control strategies for smart dampers, *Engineering Mechanics (ASCE)*, 127 (11) (2001) 1152-1164.

[22] E. A. Johnson, J. C. Ramallo, B. F. Spencer Jr and M. K. Sain, Intelligent base isolation systems, *Proc. of 2nd World Conf. on Structural Control, Wiley* (1998) 367-376.

[23] O. Yoshida and S. J. Dyke, Seismic control of a non-linear benchmark building using smart dampers, *Engineering Mechanics*, 130 (4) (2004) 386-392.

[24] C. C. Chang and L. Zhou, Neural network emulation of inverse dynamics for a magnetorheological damper, *Structural Engineering*, 128 (2) (2002) 231-239.

[25] L. Zhou and C. C. Chang, Optimal vibration control using MR dampers, *Vibration Engineering*, 15 (1) (2003) 109-113.

[26] A. Khajekaramodin, H. Haji-Kazemi, A. Rowhanimanesh and M. R. Akbarzadeh, Semi-active control of structures using neuro-inverse model of MR dampers, *Proc. of First Joint Congress on Fuzzy and Intelligent Systems*, Mashhad, Iran (2007) 789-803.

[27] K. C. Schurter and P. N. Roschke, Neuro-fuzzy modeling of a magnetorheological damper using ANFIS, *Proc. of 9th*

IEEE Int. Conf. on Fuzzy Systems, San Antonio, TX (2001) 122-127.

[28] K. K. Ahn, M. A. Islam and D. Q. Truong, Hysteresis modeling of Magneto-Rheological (MR) fluid damper by self tuning fuzzy control, *Proc. of Int. Conf. on Control, Automation and Systems*, COEX, Seoul , Korea (2008) 2628-2633.

[29] H. Wang and H. Hu, The neuro-fuzzy identification of MR damper, *Proc. of 6th Int. Conf. on Fuzzy Systems and Knowledge Discovery* (2009) 464-468.

[30] S. J. Dyke and B. F. Spencer Jr, A comparison of semi-active control strategies for the magnetorheological damper, *Proc. of IASTED Int. Conf. on Intelligent Information Systems*, (1997) 580-584.

[31] L. M. Jansen and S. J. Dyke, Investigation of non-linear control strategies for the implementation of multiple magnetorheological dampers, *Proc. of Engineering Mechanics Conference.*, *Va. (CD-ROM)* (1999).

[32] L. Hongnan, C. Zhiguo and S. Gangbing, Studies on structural vibration control with MR dampers using μGA, *Earthquake Engineering and Engineering Vibration*, 2 (4) (2005) 301-304.

[33] Y. Kim, R. Langari and S. Hurlebaus, Semi-active non-linear control of a building with a magnetorheological damper system, *Mechanical Systems and Signal Processing* (23) (2009) 300-315.

[34] Y. Q. Ni, Y. Chen, J. M. Ko and D. Q. Kao, Neuro-control of cable vibration using semi-active magnetorheological dampers, *Engineering Structures*, 24 (3) (2002) 295-307.

[35] T. Shiraishi, N. Nakaya and S. Morishita, Vibration control of structure equipped with MR damper using neural network, *Dynamics and Design Conference*, (8) (2001) 1748-1752.

[36] G. Dalei and Y. Jianqiang, Semi-active seismic isolation control based on MR damper and neural networks, *Proc. of Int. Conf. on Motion and Vibration Control*, 6 (1) (2002) 13-18.

[37] Z. Xu, Y. Shen and Guo, Semi-active control of structures incorporated with magnetorheological dampers using neural networks, *Smart Materials and Structures* (12) (2003) 80-87.

[38] L. X. Wang, *Adaptive fuzzy systems and control: design and stability analysis*, Prentice-Hall, Englewood Cliffs, NJ (1994).

[39] L. Zhou, C. C. Chang and L. X. Wang, Adaptive fuzzy control for non-linear building-magnetorheological damper system, *Structural Engineering: Special Issue on Structural Control*, 129 (7) (2003) 905-913.

[40] G. Yan and L. L. Zhou, Integrated fuzzy logic and genetic algorithms for multi-objective control of structures using MR dampers, *Sound and Vibration* (296) (2006) 368-392.

[41] S. Y. Ok, D. S. Kim, K. S. Park and H. M. Koh, Semi-active fuzzy control of cable-stayed bridges using magnetorheological dampers, *Engineering Structures* (29) (2007) 776-788.

[42] Z. D. Xu and Y. Q. Guo, Neuro-fuzzy control strategy for earthquake-excited non-linear magnetorheological structures, *Soil Dynamics and Earthquake Engineering* (28) (2008) 717-727.

[43] K. C. Schurter and P. N. Roschke, Neuro-fuzzy control of structures using magnetorheological dampers, *Proc. of the American Control Conference*, Arlington, USA (2001) 1097-1102.

[44] M. S. Daneshfard, *Semi-active vibration control of a marine structure using magnetorheological dampers*, M.S. thesis, Dept. Mechatronics. Eng., Sharif University of Technology, International Campus, Kish Island, Iran (2010).

[45] G. R. Liu and S. S. Quek, *The finite element method: A practical course,* Butterworth-Heinemann, Oxford, England (2003) 108-114.

[46] M. J. Terro, M. S. Mahmoud and M. Abdel-Rohman, Multi-loop feedback control of offshore steel jacket platforms, *Computers and Structures* (70) (1999) 185-202.

[47] J. F. Wilson, *Dynamics of offshore structures,* John Wiley & Sons, Inc, Hoboken, New Jersey, USA (2003) 28-29.

[48] M. S. Seif, *Offshore structures,* Hormozgan University Publications, Hormozgan, Iran (1997) 124-125.

[49] S. K. Chakrabarti, *Handbook of offshore engineering,* Elsevier, Plainfield, Illinois, USA, 1 (1) (2005) 91-93.

[50] K. Sadeghi, *Design of marine and offshore structures,* K. N. Toosi University of Technology Publications, Tehran, Iran (1989) 325-372.

[51] S. Chang, D. Kim, C. Chang and S. G. Cho, Active response control of an offshore structure under wave loads using a modified probabilistic neural network, *Marine Science Technology* (14) (2009) 240-247.

[52] S. Hurlebaus and L. Gaul, Smart structure dynamics, *Mechanical Systems and Signal Processing* (20) (2006) 255-281.

[53] Y. K. Wen, Method of random vibration of hysteretic systems, *Engineering Mechanics Division* (102) (1976) 249-263.

[54] R. Stanway, J. L. Spronston and N. G. Stevens, Non-linear identification of an electrorheological vibration damper, *IFAC: Identification and System Parameter Estimation* (1985) 195-200.

[55] T. T. Soong, *Active structural control: Theory and practice,* John Wiley & Sons, New York, U.S.A (1990).

[56] F. Sadek and B. Mohraz, Semi-active control algorithms for structures with variable dampers, *Engineering Mechanics* (124) (1990) 981-990.

[57] M. T. Hagan and M. B. Menhaj, Training feedforward networks with the Marquardt algorithm, *IEEE Trans. on Neural Networks*, 5 (6) (1994) 989-993.

[58] T. Takagi and M. Sugeno, Fuzzy identification of systems and its applications to modeling and control, *IEEE Trans. on Systems, Man, and Cybernetics* (15) (1985) 116-132.

[59] J. Yen and R. Langari, *Fuzzy logic: Intelligence, control, and information,* Prentice Hall, New York, NY (1999).

Atabak Sarrafan is a MSc. Student in mechatronics at Sharif University of Technology, International Campus. He was born in 1985 and also graduated in mechanical engineering in 2008 at Islamic Azad University of Ahwaz, Iran.